Bridged and cohesive crack models for fracture in composite material systems

Roberta Massabò
DICAT, University of Genova, Via Montallegro 1, 16145 Genova, Italy
roberta.massabo@unige.it

Keywords: bridged- and cohesive-crack models, fracture and delamination, scaling transitions, dynamic delamination fracture.

Abstract. The presentation reviews two modelling approaches used to study fracture in composite systems where nonlinear mechanisms arise along extended regions of the crack surfaces leading to so called large scale bridging conditions, the bridged- and the cohesive-crack models. Characteristic length scales and dimensionless groups that control fracture characteristics, size-scale transitions in the structural response of finite size members and modes of failure will be recalled and discussed. Applications to composite materials for civil, naval and aeronautical structures will be presented that highlight the significance of the bridged-crack approach in designing and optimizing new advanced composites with improved mechanical properties. Recent results on the problem of multiple dynamic delamination fracture in multilayered plates will be discussed with focus on the problem of energy absorption through multiple delamination.

Introduction

Since the early works of Barenblatt [1] and Dugdale [2], the cohesive and bridged crack models have been effectively used to model fracture in composite systems where nonlinear mechanisms arise along extended regions of the crack surfaces or ahead of pre-existing cracks (*process zones*) [3-6]. These mechanisms, which include the formation, coalescing and branching of microcracks, crazing, debonding, yielding, sliding and pulling-out of the reinforcing phases and frictional contact, can dissipate a considerable amount of energy so that additional external work is required for sustained growth of the macrocracks. Figure 1 highlights the bridging action developed by titanium short rods (z-pins) inserted to reinforce in the through-thickness direction a conventional carbon-epoxy laminate. The pins oppose the relative mode I and mode II crack displacements so shielding the crack tip from the applied load. As a consequence, the intrinsic fracture toughness of the base material is increased.

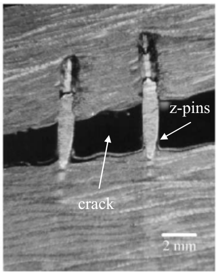

Figure 1 – Titanium z-pins bridging a mixed mode crack in a carbon-epoxy laminate (adapted from [12])

In these systems, fracture becomes a large scale bridging problem that cannot be described by Linear Elastic Fracture Mechanics or characterized by a single fracture parameter; LEFM gives a correct description of the response only in limiting configurations, where the length of the process zone is much smaller than the crack length or any other relevant lengths of the problem (e.g., the ligament size). The nonlinear crack processes must be represented explicitly in the models used to analyze the body. The bridged- and cohesive-crack models replace the process zone by a fictitious crack ahead of the pre-existing traction free crack and represent the nonlinear mechanisms as a distribution of tractions that oppose the relative crack displacements (Figure 2, for mode I problems). The tractions are related to the relative crack displacements through bridging traction laws, which aree generally nonlinear, and replace toughness and strength as the essential material properties (Figure 3 for mode I problems). The area beneath the laws define the energies supplied by the bridging or cohesive mechanisms. The bridging/cohesive traction laws can be deduced by micro- or macro-mechanics models or experiments [6,10].

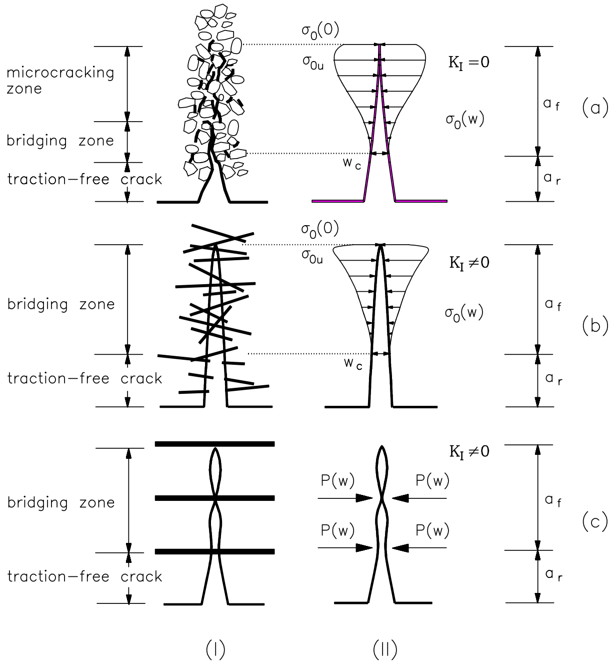

Figure 2 – Qualitative diagrams of bridging and process zones in brittle-matrix composites and quasi-brittle materials. (a) Schematic of a cohesive-crack (e.g. concrete). (b) Schematic of a crack bridged by uniformly distributed fibers (e.g. fiber-reinforced high-strength concrete, fiber reinforced ceramic matrix composite). (c) Schematic of a crack with discrete reinforcements (e.g. reinforced concrete, stitched laminate): the bridging action is well represented by localized forces [7-9]. (adapted from [5])

From a mathematical point of view, the only difference between the bridged- and the cohesive-crack model is in the form of the assumed crack tip stress field. In the *bridged crack model* this is singular (Fig. 4a) and when the crack is at the onset of growth the singular field is measured by an intrinsic fracture toughness, $K_{\mathrm{I}} = K_{\mathrm{IC}}$, or fracture energy, $\mathcal{G}_{\mathrm{I}} = \mathcal{G}_{\mathrm{IC}} = K_{\mathrm{IC}}^2 / E$, with E a representative Young's modulus (for mode I problems). In the *cohesive crack model*, the crack tip stress field is finite (non singular) and when the crack is at the onset of propagation the stress normal to the crack plane at the crack tip equals the value of the cohesive tractions at zero displacement (Fig. 4b). In this sense the cohesive-crack model can be considered as a particularization of the bridged-crack model under the assumption of a vanishing crack tip stress-intensity factor or a vanishing intrinsic fracture toughness, $K_{\mathrm{I}} = K_{\mathrm{IC}} = 0$. However, the two models are conceptually different as they presuppose different descriptions of the material leading to a different significance of the bridging tractions.

In the *bridged-crack model*, the composite is theoretically simulated as a biphase material and two distinct factors contribute to its global toughness: the toughness peculiar to the matrix, described by K_{IC} or $\mathcal{G}_{\mathrm{IC}}$ (for mode I problems), and the secondary phase toughening mechanism, which is represented by the shielding effect that the bridging tractions develop on the crack tip stress field and described by $\mathcal{G}_{\mathrm{b}} = \int_0^{w_{\mathrm{c}}} \sigma_0(w)dw$ (for a mode I problem). Crack growth is governed by the intrinsic toughness of the matrix and the bridging tractions, which control relative crack displacement, are governed by the properties of the reinforcing phase and by its interaction with the matrix. The bridged-crack model is then suitable for the description of separation processes that involve distinct physical phenomena (crack tip toughness + shielding), such as those of through-thickness reinforced laminates, fiber reinforced high strength concrete or reinforced concrete.

In the *cohesive-crack model*, the composite material is theoretically simulated as being homogeneous. Only the global toughening mechanism of the whole composite is defined, and it is represented by the shielding effect due to the cohesive tractions. The toughening mechanism peculiar to the matrix and explicitly represented in the previous model by $\mathcal{G}_{\mathrm{IC}}$, is now merged with the toughening mechanisms developed in the process zone through the cohesive law and defined by $\mathcal{G}_{\mathrm{b}}$. The damage process producing the growth of the crack is the same as that governing relative crack displacement along the process zone. The model is suitable to describe the separation process of materials characterized by a wide zone of microcracking, plastic deformation or crazing, when the matrix toughness is negligible compared to the energy dissipated in the nonlinear processes. However, the definition of appropriate cohesive laws (e.g. a two-part law, Fig. 3d) allows utilization of the cohesive-crack model in the description of materials characterized by distinct mechanisms of crack control.

The mutual relations of the two models have been examined in [5,11] and will be discussed in the presentation.

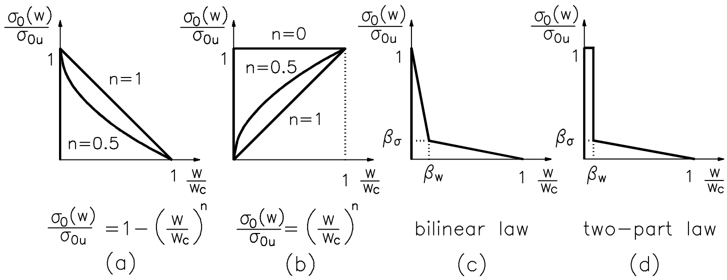

Figure 3 – Exemplary bridging and cohesive traction laws representing different nonlinear mechanisms: (a) pull out of short fibers or rods; (b) progressive debonding and yielding of continuous fibers; (c)-(d) cohesive mechanisms in concrete like materials and fiber reinforced concrete (adapted from [5])

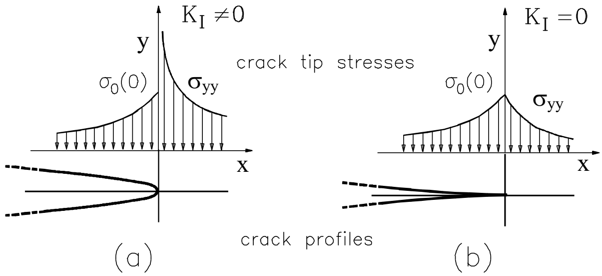

Figure 4 - Conditions at the crack tip - (a) bridged-crack model: crack tip profile determined by LEFM; (b) cohesive-crack model: smooth closure of the crack surfaces (adapted from [5]).

Characteristic length scales and brittleness numbers

The nature of the crack and the structure behavior of quasi-brittle materials and brittle-matrix composites can range from stable to unstable depending on material properties, structure geometry, loading conditions and external constraints. In particular, the mechanical response is not physically similar when the size scale of the body is varied. The two limiting solutions, given by Linear Elastic Fracture Mechanics and by the perfectly-plastic limit analysis may be used only for extremely brittle cases and for extremely ductile cases, respectively. The intermediate cases must be analyzed by resorting to a cohesive- or bridged-crack approach.

Material brittleness and ductility

A first indication of the fracture behavior expected in a given material is provided by the length of the process zone of a crack propagating in small-scale bridging conditions in a uniformly loaded infinite medium, l_{SSB} (Fig. 5a). *Small-scale bridging* fracture is approached when the process zone evolves to a zone of constant length, much smaller than the length of the crack, the fracture toughness becomes a constant and the solution of the problem approaches that expected for a brittle crack (LEFM) when the material toughness includes the work required to fail the ligaments (Fig. 5b). Using the model parameters defined in Fig. 3, for a rectangular bridging or cohesive law ($\sigma_0(w)=\sigma_{0u}$ for $w \le w_c$ and $\sigma_0(w)=0$ for $w > w_c$), this length is a material property given by:

$$l_{\mathrm{SSB}} = \frac{\pi}{8}\frac{w_c E}{\sigma_{0u}} \quad , \tag{1}$$

for a cohesive crack with vanishing intrinsic fracture toughness [13], and

$$l_{\mathrm{SSB}} = \frac{\pi}{8}\frac{w_c E}{\sigma_{0u}}\left(\sqrt{1+\frac{\mathcal{G}_{\mathrm{IC}}}{\mathcal{G}_{\mathrm{b}}}} - \sqrt{\frac{\mathcal{G}_{\mathrm{IC}}}{\mathcal{G}_{\mathrm{b}}}}\right)^2 , \tag{2}$$

for a bridged crack [14]. The factor $\pi/8$ changes on varying the shape of the cohesive/bridging law but it remains of order unity. The length of the process zone in the small scale bridging limit characterizes the *intrinsic brittleness of the material*; its order of magnitude is equal to 10^{-6} mm in glass, 10^{-3} mm in ceramic-matrix ceramic-fiber composites, $10^0 \div 10^1$ in conventional 2D laminates and $10^2 \div 10^3$ mm in concrete, fiber-reinforced cementitious materials and through-thickness reinforced laminates.

The size of the cohesive/bridged zone depends on the groups $w_c E/\sigma_{0u}$ and $\mathcal{G}_{IC}/\mathcal{G}_b$. The dimensional group $w_c E/\sigma_{0u}$, which alone defines the process zone length in a cohesive crack model of the material, was first noted by Cottrell [15] as the material parameter correlating notch sensitivity of ultimate strength to notch size, and reconsidered by Hillerborg in its definition of the characteristic length, l_{ch}, to describe concrete like materials [16].

The second dimensionless group, $\mathcal{G}_{IC}/\mathcal{G}_b$, is the ratio between the intrinsic fracture energy and the energy supplied by the bridging mechanisms; it appears in the definition of the small scale bridging process zone length when a bridged-crack approach is used and indicates a progressive transition toward material brittleness when $\mathcal{G}_{IC}/\mathcal{G}_b$ increases. The length scale Eq. (1) defines an upper bound solution to the length of the process zone for $\mathcal{G}_{IC}/\mathcal{G}_b \to 0$.

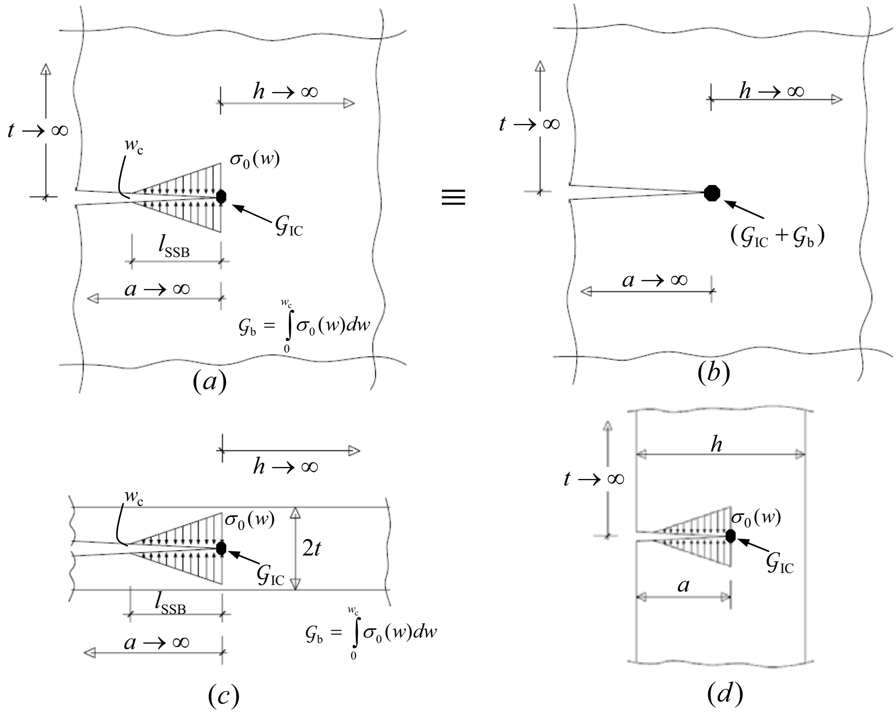

Figure 5 - Schematics of bridged cracks: (a) fracture process zone in small scale bridging conditions; (b) LEFM approximation of small scale bridging fracture; (c) small scale bridging limit in a slender body; (d) large scale bridging fracture in a member of finite size.

In slender bodies, such as delamination beams (Fig. 5c), the length of the process zone in small scale bridging becomes a material/structure parameter that scales with the thickness $2t$ of the body and the scaling rule depends on the mode of fracture. The characteristic length scales for slender bodies have been derived in [17] and [18] and are given by:

$$l_{SSB}^{I} \approx (l_{SSB})^{1/4} t^{3/4} \quad \text{for mode I fracture in a slender body} \tag{3}$$

$$l_{\mathrm{SSB}}^{\mathrm{II}} \approx (l_{\mathrm{SSB}} t)^{1/2} \quad \text{for mode II fracture in a slender body} \tag{4}$$

where l_{SSB} is given in Eqs. (1) and (2).

In members subjected to uniform loading conditions and when the bridging traction law is an increasing function of the relative crack displacement (at least over a certain interval), a second limiting configuration can be approached, the *ACK limit* (from the seminal work of Avenston, Cooper and Kelly [19]). In this limit, which is characterized by a long crack entirely bridged by intact ligaments and is typically reached after the crack has grown several time a non-catastrophic characteristic length scale, l_{ACK}, the critical load for crack propagation becomes constant. The ACK characteristic length scales for infinite and slender bodies have been derived in [14] and [18]. For a prescribed mode I power bridging law, $\sigma_0(w_{\mathrm{N}}) = \beta(w_{\mathrm{N}}/2)^{\alpha}$, in an infinite body, l_{ACK} is a material property given by:

$$l_{\mathrm{ACK}} = \frac{\pi E}{4}\left(\frac{1+\alpha}{2\alpha}\mathcal{G}_{\mathrm{Ic}}\right)^{\frac{1-\alpha}{1+\alpha}} \beta^{\frac{-2}{1+\alpha}}. \tag{5}$$

and for a centered mode II crack in a slender beam of half thickness t, with a power bridging law, $\tau_0(w_{\mathrm{S}}) = \beta(w_{\mathrm{S}}/2)^{\alpha}$, l_{ACK} is a material/structure property given by:

$$l_{\mathrm{ACK}}^{\mathrm{II}} \approx (l_{\mathrm{ACK}} t)^{1/2}. \tag{6}$$

Whether crack propagation across a long and unnotched member ($h >> l_{\mathrm{SSB}}, l_{\mathrm{ACK}}$) will be noncatastrophic (no ligament failure - ACK limit attainable) or catastrophic (extensive ligament failure - small scale bridging limit approached) can be estimated by comparing the orders of magnitude of l_{SSB} and l_{ACK}. If $l_{\mathrm{ACK}} >> l_{\mathrm{SSB}}$, failure will be catastrophic; if $l_{\mathrm{SSB}} >> l_{\mathrm{ACK}}$, noncatastrophic. The presence of a notch favours catastrophic cracking. If neither limit can be approached (e.g., $l_{\mathrm{SSB}} \approx l_{\mathrm{ACK}}$ or $h \approx l_{\mathrm{ACK}}$ or $h \approx l_{\mathrm{SSB}}$) then large-scale bridging conditions prevail and detailed calculations are required. Figure 6 highlights failure transitions in a delamination beam subject to pure mode II conditions where the last condition applies.

Structure brittleness and ductility

To describe the fracture response of finite size bodies (Fig. 5d), dimensionless groups that depend on l_{SSB} and a characteristic dimension of the members (e.g., h in Fig. 5d) have been proposed. To describe the response of concrete structures ($K_{\mathrm{IC}} = 0$), Hillerborg *et al.* [16] used the dimensionless group l_{SSB}/h, which was also considered by Bao and Suo [3] to describe notch and hole sensitivity in ceramic and metal matrix composites, with h the notch or radius length. Carpinteri [20] introduced the energy brittleness number,

$$s_{\mathrm{E}} = \frac{\mathcal{G}_{\mathrm{b}}}{\sigma_{0\mathrm{u}} h}, \tag{7}$$

as the parameter that synthetically controls the fracture behavior of elasto-softening materials (K_{I}=0) and the size-scale transition from ductile to brittle response of geometrically similar structures loaded in flexure (note that $s_{\mathrm{E}}/\varepsilon_{\mathrm{u}} = l_{\mathrm{SSB}}$, ε_{u} being the ultimate elastic strain of the composite). Physical similarity is found in the structural response if the parameter s_{E} is kept constant, and physical non-similarity is found when s_{E} varies, due for instance to variations in h; a transition from ductile to brittle responses is predicted when s_{E} decreases.

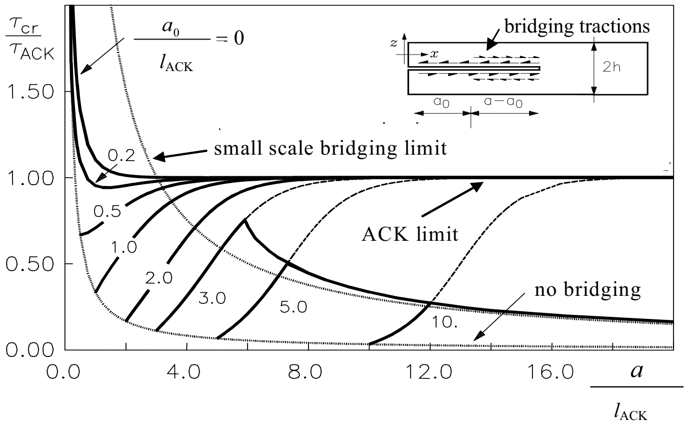

Figure 6 - Transition from noncatastrophic (ACK limit approached, $\tau = \tau_{cr} = \tau_{ACK}$) to catastrophic (small scale bridging limit approached) failure on varying the notch length, a_0, in a stitched plate subject to uniformly distributed shear stresses, τ, acting along the crack surfaces. The problem is pure mode II and the bridging law is linear and non proportional ($\tau_0(w_S) = \tau_0(0) + \beta w_S / 2$ with $\tau(0) = 2\sqrt{\mathcal{G}_{IIC}\beta}$ and $\mathcal{G}_b / \mathcal{G}_{IIC} = 80$). The critical stress for crack propagation in the ACK limit is a material property, $\tau_{ACK} = 3(\mathcal{G}_{IIC}\beta)^{1/2}$, and the characteristic length scale l_{ACK} a material structure property $l_{ACK} = [E/(4\beta)t]^{1/2}$ [18]. For the stitched laminate tested in [10] with $2t$ = 7 mm, E = 49 GPa, $\tau_0(w_S) = 12.7 + 51 w_S$ MPa and w_c = 1.0 mm, $l_{ACK} \approx 20$ mm and $l_{SSB} \approx 40$ mm (adapted from [10]).

A single dimensionless parameter also controls the structural brittleness of brittle-matrix composites ($K_{IC} \neq 0$) characterized either by an increasing bridging relationship or by a rigid-perfectly plastic relationship (Fig. 3b with $w_c \to \infty$). In these materials the length of the bridged zone progressively increases during crack propagation. Carpinteri et al. [7,8] introduced the brittleness number N_P as the parameter that controls the flexural failure and the transition from ductile to brittle behavior in reinforced concrete:

$$N_P = \frac{\rho \sigma_u h^{0.5}}{K_{IC}}, \tag{8}$$

where ρ is the reinforcement ratio, σ_u is the minimum of the reinforcement stresses at the yielding and sliding limits, and h is the depth of the member (Fig. 5d). The same parameter describes the structural behavior of brittle matrix composites reinforced with uniformly distributed ductile reinforcements [9]. The product $\rho\sigma_u$ defines the ultimate bridging stress, σ_{0_u} (Fig. 3b).

On the other hand, the structural behavior of brittle-matrix composites ($K_{IC} \neq 0$) characterized by a bridging law with a critical value of the crack opening displacement, w_c, beyond which the bridging tractions vanish, is controlled by two dimensionless parameters, given for instance by l_{SSB}/h or s_E or N_P and $\mathcal{G}_{IC}/\mathcal{G}_b$.

The dimensionless groups, l_{SSB}/h and $\mathcal{G}_{IC}/\mathcal{G}_b$, have been used in the description of notch and hole sensitivity of ultimate strength in brittle and metal matrix composites (see [3]); s_E or N_P and $\mathcal{G}_{IC}/\mathcal{G}_b$ have been used in [5,11,21] to study the flexural failure of brittle matrix composites and compare the bridged-crack approach with the cohesive-crack approach in the structural analyses of flexural members. Figure 7 depicts failure transitions in flexural members [11].

In the presentation, the concepts summarized in this section will be reviewed and applications will be presented that highlight scaling transitions in different materials and systems.

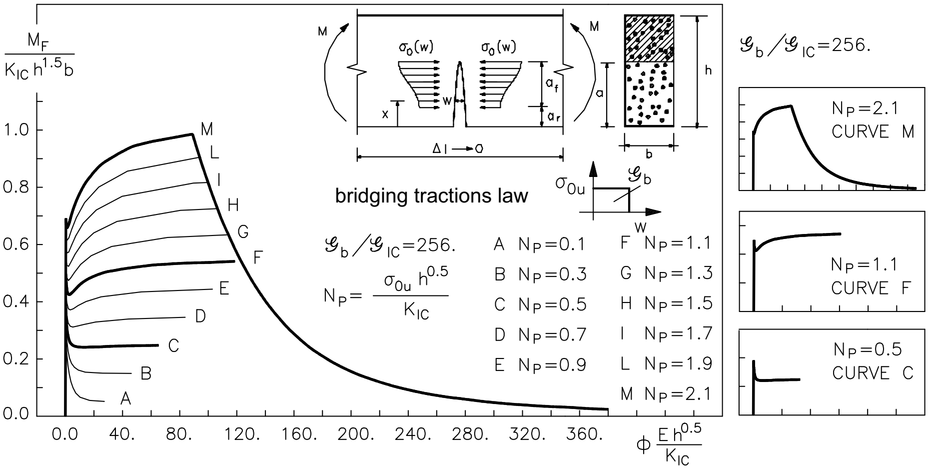

Figure 7 - Double brittle-ductile-brittle transition in the flexural response of a brittle-matrix composite with intrinsic fracture toughness K_{IC} reinforced with uniformly distributed discontinuous fibers (rectangular bridging law $\sigma_0(w)=\sigma_{0u}$ for $w \le w_c$; $\sigma_0(w)=0$ for $w > w_c$, with w_c a critical crack opening displacement). The dimensionless moment versus bending rotation constitutive response is controlled by two dimensionless parameters: the brittleness number $N_P=\sigma_{0u}h^{0.5}/K_{IC}$ [11,9] and $\mathcal{G}_b/\mathcal{G}_{IC}$. For a cementitions material reinforced with steel fibers with K_{IC} = 50 N/mm$^{1.5}$, E = 40 GPa, σ_{0u} = 4 MPa and w_c = 4 mm (leading to $\mathcal{G}_b/\mathcal{G}_{IC}$ =256), the curves labeled C, F and M describe the response of beams with depths $h \sim 40$ mm, $h \sim 190$ mm and $h \sim 690$ mm, respectively. The depths of the first two beams are in the range normally covered by the laboratory specimens and in this range a brittle-ductile transition is typically observed when the beam depth increases [22]. However, in the steel fiber reinforced composite examined here, a new ductile-brittle transition is predicted when the beam depth further increases above the transitional value given by the curve F, and the largest beam (curve M), which could represent a real structural component, is characterized by an unstable response. For larger/smaller values of the ratio $\mathcal{G}_b/\mathcal{G}_{IC}$, the critical value of N_P beyond which the response changes from globally stable to globally unstable increases/decreases and the reversal is not present when the bridging traction law is rigid-perfectly plastic ($w_c \to \infty$). The diagram has been obtained with the bridged-crack model formulated in [11].

Modeling large scale bridging delamination fracture for the design of advanced composites

The bridged- and cohesive-crack models have been used in the recent past [6,18,23-30] by the author and her collaborators to study single and multiple, quasi-static and dynamic delamination fracture in multilayered plates. In the presentation, results will be reviewed that highlight the significance of the bridged-crack approach in designing and optimizing new advanced composites with improved mechanical properties (e.g. laminates reinforced with a through-thickness reinforcement such as stitching or z-pinning).

The problem of multiple delamination fracture, which is the typical outcome of extreme dynamic loading conditions, such as high velocity impact and blast, will also be examined. The effects of the interaction between delaminations and of nonlinear crack face mechanisms, including bridging by fibers and through-thickness reinforcements, contact and friction, on fracture characteristics, macrostructural response, damage and impact tolerance and energy absorption will be discussed. Damage/impact tolerance can be substantially improved by adding a through-thickness reinforcement [10,6] and recent results indicate that energy absorption through multiple delamination fracture can be optimized if the system is designed so that cracks will form at predefined spacing [27,30]. Figure 8 highlights these behaviors.

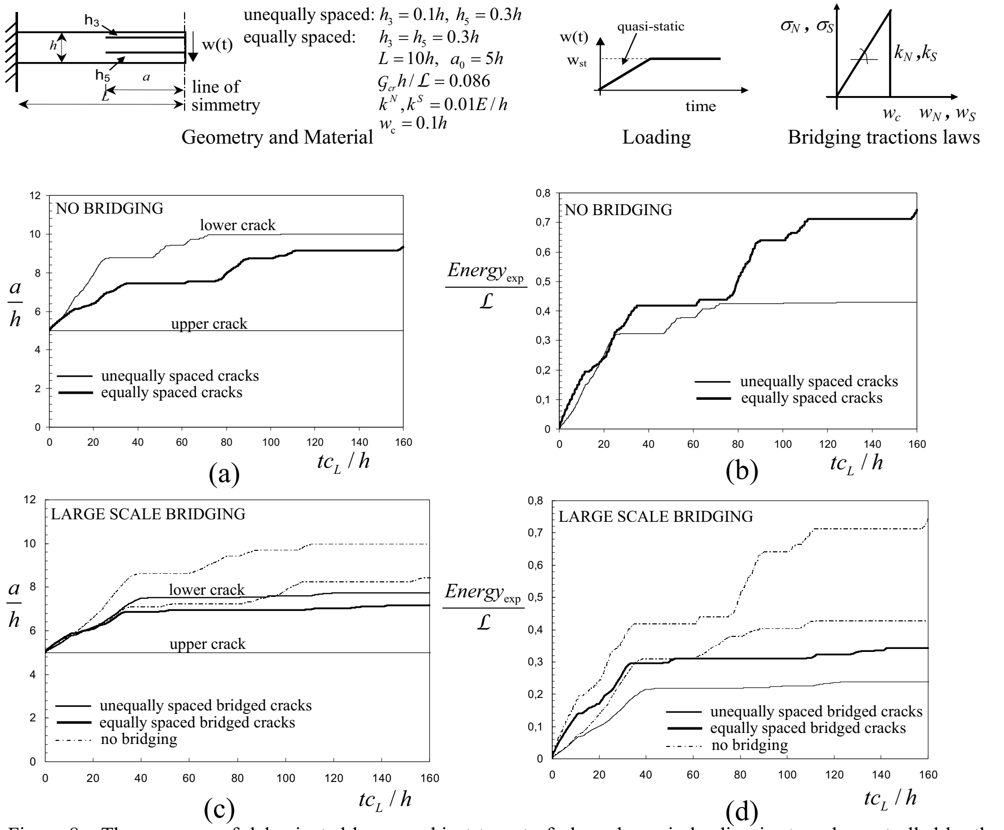

Figure 8 - The response of delaminated beams subject to out of plane dynamic loading is strongly controlled by the crack spacing, the material layup and the presence of large scale bridging conditions [27]. This figure depicts results on damage tolerance and energy absorption through multiple dynamic delamination fracture in homogeneous systems. Two delaminated clamped-clamped beams with equally and unequally spaced, central and traction free cracks have been loaded quasi-statically up to predefined values of the mid-span displacement w_{st} that ensure a fixed value of the strain energy, $\mathcal{L}$, in the systems. Crack growth was prevented during the static loading. The cracks were then allowed to propagate dynamically through the specimens with the mid-span displacement kept fixed at w_{st} (fracture criterion: $\mathcal{G} \geq \mathcal{G}_{cr}$ with $\mathcal{G}$ the energy release rate and $\mathcal{G}_{cr}$ the intrinsic fracture energy of the base material). The strain energy introduced into the two systems was such that crack growth occurred in the regime of small to moderate crack speeds. Diagrams (a-b) refer to the unreinforced beams; diagrams (c-d) refer to the reinforced beams in the presence of large scale bridging mechanisms described by linear proportional bridging laws that could represent a stitched laminate (the bridging mechanisms act in the initially intact ligaments of the beams). The diagrams highlight important features of the response of these systems. – In both the reinforced and the unreinforced systems, (a) and (c), the equally spaced cracks propagate together (at a speed of approximately $0.1c_L$, with c_L the longitudinal wave speed); in the unequally spaced system only the lower crack propagates and in the unreinforced system single growth occurs at much higher speed (approximately $0.2c_L$) and the crack quickly approaches the fixed boundary of the member. – The large scale bridging mechanisms reduce crack speed in the unequally spaced system and, after a phase of growth at reduced speed, lead to crack arrest in both systems; this indicates that the damage and impact tolerance of the material can be substantially improved by a through-thickness reinforcement when crack growth occurs in the low to moderate crack speed regime [24]. – In the unreinforced systems, the energy expended into the creation of new surfaces, (b), is much higher when both cracks propagate suggesting that if the beams were designed so that cracks will form at equal spacing, energy absorption through multiple delamination fracture could be optimized. – The presence of large scale bridging conditions minimizes differences in the responses of the systems with equally and unequally spaced cracks. (results obtained with the cohesive interface model formulated in [27,28]).

Conclusions

The presentation reviews basic concepts of the theory of crack bridging, with special focus on length scales and dimensionless groups that control fracture characteristics, size-scale transitions in the structural response and modes of failure of members of finite size and slender bodies. Recent results on static and dynamic single and multiple delamination fracture will be presented that highlight the significance of the bridged-crack approach in designing and optimizing new advanced composite materials and structures with improved mechanical properties.

Acknowledgements: Support by the U.S. Office of Naval Research through contract no. N00014-05-1-0098, administered by Dr. Yapa D.S. Rajapakse is gratefully acknowledged.

References

[1] Barenblatt, G.I., (1959), The formation of equilibrium cracks during brittle fracture. General ideas and hypotheses. Axially-symmetric cracks, *J. Applied Mathematics and Mechanics* 23, 622-636.
[2] Dugdale, D.S., (1960), Yielding of steel sheets containing slits, *J. Mechanics Physics Solids* 8, 100-104.
[3] Bao, G., and Suo, Z. (1992), Remarks of crack-bridging concepts, *Applied Mechanics Review* 24, 355-366
[4] Cox, B.N., and Marshall, D.B. (1994) Concepts for bridged cracks in fracture and fatigue. *Acta Metall. Mater.*, 42, 341-363.
[5] Massabò, R., (1999), The bridged-crack model, in *Nonlinear Crack Models for Nonmetallic Materials*, (ed. A. Carpinteri), Solid Mechanics and its Applications Series (ed. G. Gladwell), Kluwer Academic Publisher (ISBN 0-7023-5750-7), Dordrecht, The Netherlands, pp. 141-208.
[6] Massabò, R. (2008), Single and multiple delamination in the presence of nonlinear crack phase mechanisms, book chapter in *Delamination Behavior of Composites*, (Ed. Sridharan), Woodhead Publishing Ltd., Cambridge, UK, pp. 1-51, ISBN: 978-1-84569-244-5, in press.
[7] Carpinteri, A., Stability of fracturing process in r.c. beams: *J. Structural Engineering* 110 (1984), 544-558.
[8] Bosco, C., and Carpinteri, A.: Discontinuous constitutive response of brittle matrix fibrous composites, *J. Mechanics Physics Solids* **43** (1995), 261-274.
[9] Carpinteri, A., and Massabò, R. (1997) Continuous versus discontinuous bridged crack model for fiber-reinforced materials in flexure, *Int. Journal of Solids and Structures*, 34(18), 2321-2338.
[10] Massabò, R., Mumm, D., and Cox, B.N., (1998) Characterizing mode II delamination cracks in stitched composites*, Int. Journal of Fracture*, 92(1), 1-38
[11] Carpinteri, A., and Massabò, R. (1996) Bridged versus cohesive crack in the flexural behavior of brittle matrix composites, *Int. Journal of Fracture*, 81, 125-145.
[12] Rugg, Cox, & Massabò, 2002, Mixed mode delamination of polymer composite laminates reinforced through the thickness by z-fibers, *Composites*, *part A*, **33**/2, 177-190.
[13] Bilby, B.A., Cottrell, A.H., and Swinden, K.H., (1963), The spread of plastic yield from a notch, *Proceedings Royal Society London* **A272**, 304-314
[14] Marshall, D.B., Cox, B.N., and Evans, A.G.: The mechanics of matrix cracking in brittle-matrix fiber composites, *Acta Metallurgica Materialia* **33** (1985), 2013-2021.
[15] Cottrell, A.H., (1963), Mechanics of Fracture, in *Tewksbury Symposium of Fracture,* University of Melbourne, Australia, 1-27.

[16] Hillerborg, A., Modeer, M., and Petersson, P.E., (1976), Analysis of crack formation and crack growth in concrete by means of fracture mechanics and finite elements, *Cement and Concrete Research* **6**, 773-782.
[17] Suo, Z., Bao, G., and Fan, B. (1992), Delamination R-Curve phenomena due to damage, *J. Mech. Phys. Solids*, 40, 1-16.
[18] Massabò, R., and Cox, B.N., (1999), Concepts for bridged mode II delamination cracks, *Journal of the Mechanics and Physics of Solids*, 47(6), 1265-1300
[19] Aveston, J., Cooper, G.A., and Kelly, A. (1971) Single and multiple fracture. In *The properties of fiber composites*, Conf. Proc., National Physical Laboratory, IPC Science and Technology Press Ltd., 15-24.
[20] Carpinteri, A.: Cusp catastrophe interpretation of fracture instability, J. Mechanics Physics Solids 37 (1989), 567-582.
[21] Carpinteri, A., and Massabò, R. (1997) Reversal in the failure scaling transition of brittle matrix fibrous composites, *Journal of Engineering Mechanics (ASCE),* 123(2), 107-114.
[22] Jenq, Y.S., and Shah, S.P.: Crack propagation in fiber-reinforced concrete, *J. Structural Engineering* **112** (1986), 19-34.
[23] Massabò, R., and B.N. Cox (2001), Unusual characteristics of mixed mode delamination fracture in the presence of large scale bridging, *Mechanics of Composite Materials and Structures*, **8**(1), 61-80
[24] Sridhar, N., Massabò, R., Cox, B.N., and Beyerlein, I., (2002) Delamination dynamics in through-thickness reinforced laminates with application to DCB specimen, International Journal of Fracture, 118, 119-144.
[25] Andrews, M.G., Massabò, R., and Cox, B.N., (2006) Elastic interaction of multiple delaminations in plates subject to cylindrical bending, International Journal of Solids and Structures, 43(5), 855-886.
[26] Andrews, M.G. and Massabò, R., (2008) Delamination in flat sheet geometries in the presence of material imperfections and thickness variations, *Composites Part B*, 39, 139-150, special issue on Marine Composites.
[27] Andrews, M.G., Massabò, R., Cavicchi, A., Cox, B.N., 2008, Dynamic interaction of multiple delaminations in plates subject to cylindrical bending, submitted.
[28] Andrews, M.G. (2005), *The Static and Dynamic Interaction of Multiple Delaminations in Plates Subject to Cylindrical Bending*, Dissertation, Ph.D. Degree, Northwestern University, Evanston, IL, U.S.A..
[29] Massabò R., and Cavicchi, A., (2007) Influence of crack wake mechanisms on the dynamic fracture of multiply delaminated plates, proceedings of the 16th Int. Conference on Composite Materials, ICCM16, Kyoto, July 2007, CDrom pp. 1-7, Japan Society of Composite Materials.
[30] Massabò R., (2007) Dynamic interaction of multiple damage mechanisms in multilayered systems, proceedings of the XVIII *National Congress of the Italian Association of Theoretical and Applied Mechanics*,, AIMETA2007, Brescia, September 2007, pp. 1-12, CDROM.